

BLIND CFO ESTIMATION IN OFDM SYSTEMS USING DIAGONALITY CRITERION

Timo Roman, Visa Koivunen

SMARAD CoE, Signal Processing Laboratory
Helsinki University of Technology
P.O. Box 3000, FIN-02015 HUT, Finland

ABSTRACT

In this paper we address the problem of blind carrier frequency offset (CFO) estimation in OFDM systems in the case of frequency selective channels. By assuming real constellations, the proposed blind method enforces a diagonal structure for signal pseudo-covariance matrices in frequency domain. Power of non-diagonal elements is minimized. A closed-form solution is derived which leads to accurate and computationally efficient CFO estimation in multipath fading channels. Moreover, in case of complex circularly symmetric noise, the theoretical performance does not depend on the SNR. Simulation results are presented using realistic channel model in typical urban scenarios.

1. INTRODUCTION

Orthogonal Frequency Division Multiplexing (OFDM) modulation has already proven successful for both wireless (e.g. DVB-T and WLAN) and wireline applications (e.g. ADSL). Multicarrier modulations are a powerful technique to handle impairments of wireless communication media such as multipath propagation, due to their ability to turn frequency selective channels into a set of narrow-band frequency flat channels. Hence, OFDM is a viable candidate for future beyond 3G wireless communications standards.

One of the main drawbacks of OFDM is its high sensitivity to frequency offsets caused by the oscillator inaccuracies and the Doppler shift due to mobility, giving rise to inter-carrier interference (ICI). This issue is critical when higher data rates are required, and relatively large number of subcarriers and very narrow guard bands are used. Consequently, frequency offset estimation must be accomplished with high fidelity.

The ICI resulting from carrier offset can be compensated in several ways. One may perform frequency offset estimation and then offset compensation [1, 4, 7] or can compensate directly for the offset [3]. Both approaches can be applied in a blind manner [3, 7] or by using training symbols [1]. Several blind methods rely on examining the correlation of the received signal [2, 5, 7]. The method in [2] investigates the diagonal elements of the correlation matrix of the received signal. Methods proposed in [5, 7] use cross-correlations between successive received blocks and require a specific preprocessing stage, assuming redundancies in the transmitted symbols or blocks. Unfortunately, they lead up to 50% decrease of the effective data rate. Blind frequency offset compensation has been also addressed in [4] based on the diagonal elements of signal pseudo-covariance matrix assuming AWGN channel.

This work was supported by the Academy of Finland. Helpful comments from Jan Eriksson and Dr Mihai Enescu are gratefully acknowledged.

In this paper, a method for CFO estimation and compensation in frequency selective channels is introduced. The method is blind since it does not require a priori knowledge of the transmitted data or the multipath channel. A cost function minimizing the total off-diagonal power induced by ICI in received signal pseudo-covariance matrix is derived. Enforcing a diagonal structure leads to perfectly frequency synchronized OFDM transmission. The proposed method assumes that real constellations are used. This allows embedding the frequency offset in the cost function. In addition, the theoretical performance of the estimator becomes independent of the signal-to-noise ratio (SNR) in the face of complex circularly symmetric noise. Hence it enables accurate CFO estimation at low SNR regime, where decision-directed methods are most likely to fail. A closed-form expression is found for the cost function which leads to low complexity and accurate computational solution.

The rest of the paper is organized as follows. The system model is briefly described next. In Section 3, we define the cost function and derive a new blind frequency offset estimation algorithm. In Section 4, we demonstrate the reliable performance of the proposed method in simulations using realistic channel model and different noise levels. Finally, Section 5 concludes the paper.

2. SYSTEM MODEL

2.1. Input-output relationships

The OFDM transmission model used in this paper is presented in Figure 1. As the cyclic prefix provides us with inter-block inter-

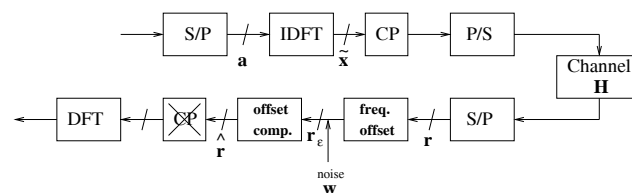


Fig. 1. OFDM transmission chain.

ference free transmission, we can process each OFDM block independently. The k^{th} modulated OFDM block is written as $\tilde{x}(k) = \mathbf{F}_N \mathbf{a}(k)$, where \mathbf{F}_N is the $N \times N$ inverse discrete Fourier transform (IDFT) matrix, N being the total number of subcarriers and $\mathbf{a}(k)$ is the $N \times 1$ complex symbol vector.

The $P \times 1$ signal block after cyclic prefix insertion, followed by transmission on the wireless channel (Figure 1) is expressed as:

$$\mathbf{r}(k) = \mathbf{H} \mathbf{T}_{CP} \tilde{\mathbf{x}}(k), \quad (1)$$

where \mathbf{H} is the Toeplitz channel convolution matrix of size $P \times P$ and the $P \times N$ matrix \mathbf{T}_{CP} adds a cyclic prefix of length L . Consequently $P = N + L$ is the total OFDM block size. The channel taps $\{h_l\}_{l=0, \dots, L_h-1}$ contained in \mathbf{H} are assumed to be time-invariant. The channel is considered to have a maximum of L_h taps, hence it is frequency selective. The length of the cyclic prefix is $L \geq L_h$ in order to avoid inter-block interference.

Let us now assume the received signal is subject to a frequency deviation ϵ , a single parameter to be estimated. The quantity ϵ chosen as $0 \leq \epsilon < 1$, is referred to as normalized frequency offset. Thus, effective frequency deviation lies within the interval $[0, B/N]$, where B is the total bandwidth allocated to the system. Hence, the received $P \times 1$ block with frequency offset is:

$$\mathbf{r}_\epsilon(k) = \mathbf{C}_\epsilon \mathbf{r}(k) + \mathbf{w}(k), \quad (2)$$

where \mathbf{C}_ϵ is the $P \times P$ frequency offset diagonal matrix having the form:

$$\mathbf{C}_\epsilon = \text{diag}\{\mathbf{c}_\epsilon\}, \quad (3)$$

with $\mathbf{c}_\epsilon = [1, \exp(j2\pi\epsilon/N), \dots, \exp(j2\pi(P-1)\epsilon/N)]^T$. The complex noise term \mathbf{w} in (2) is assumed to be proper complex Gaussian [6].

2.2. Frequency offset compensation

Given an estimate $\hat{\epsilon}$ of the true value ϵ , frequency offset can be compensated for at the receiver in the following way:

$$\mathbf{r}_{\hat{\epsilon}\epsilon}(k) = \mathbf{C}_{\hat{\epsilon}}^* \mathbf{r}_\epsilon(k) \quad (4)$$

$$= \mathbf{C}_{\hat{\epsilon}}^* \mathbf{C}_\epsilon \mathbf{r}(k) + \mathbf{C}_{\hat{\epsilon}}^* \mathbf{w}(k), \quad (5)$$

where (5) follows from (2), $\mathbf{C}_{\hat{\epsilon}}$ has the structure defined in (3), and $*$ denotes the complex conjugation operation.

After cyclic prefix removal followed by DFT on (4), we obtain the vector:

$$\tilde{\mathbf{r}}_{\hat{\epsilon}\epsilon}(k) = \mathbf{F}_N^H \mathbf{R}_{CP} \mathbf{r}_{\hat{\epsilon}\epsilon}(k) = \mathbf{F}_N^H \mathbf{R}_{CP} \mathbf{C}_{\hat{\epsilon}}^* \mathbf{r}_\epsilon(k), \quad (6)$$

where the matrix $\mathbf{R}_{CP} = [\mathbf{0}_{N \times L} \quad \mathbf{I}_N]$ is used to remove the cyclic prefix.

3. BLIND FREQUENCY OFFSET ESTIMATION

3.1. Signal pseudo-covariance matrix structure

Let us first define the pseudo-covariance matrix of the signal in time-domain as follows:

$$\mathbf{R}_\epsilon \triangleq \mathbb{E} \left[\mathbf{r}_\epsilon(k) \mathbf{r}_\epsilon^T(k) \right], \quad (7)$$

where $\mathbb{E}[\cdot]$ is the expectation operator. The justification to employ pseudo-covariance instead of the commonly used covariance is that it vanishes for proper complex random variables such as the noise term \mathbf{w} , but the information on the frequency offset ϵ is retained. Consequently, the proposed method applies to real constellations.

Starting from equations (1) and (2), we express (7) as:

$$\begin{aligned} \mathbf{R}_\epsilon &= \mathbf{C}_\epsilon \mathbf{H} \mathbf{T}_{CP} \mathbf{F}_N \mathbb{E}[\mathbf{a}(k) \mathbf{a}^T(k)] \mathbf{F}_N^T \mathbf{T}_{CP}^T \mathbf{H}^T \mathbf{C}_\epsilon^T + \\ &\quad \mathbb{E}[\mathbf{w}(k) \mathbf{w}^T(k)]. \end{aligned} \quad (8)$$

In the following, we assume unit power independent BPSK symbols, leading to $\mathbb{E}[\mathbf{a}(k) \mathbf{a}^T(k)] = \mathbf{I}$ and circular white Gaussian noise with variance σ^2 , which implies $\mathbb{E}[\mathbf{w}(k) \mathbf{w}^H(k)] = \sigma^2 \mathbf{I}$, and $\mathbb{E}[\mathbf{w}(k) \mathbf{w}^T(k)] = \mathbf{0}$. In theory, the pseudo-covariance of the noise vanishes on average. Hence the performance of the algorithm should not depend on the SNR if noise is circularly symmetric. However in practice, the sample estimates of the pseudo covariance matrix experience perturbations because of noise.

Let us consider compensation for the carrier offset as defined in (4). It is followed by cyclic prefix removal and DFT. Consequently, the pseudo-covariance matrix $\tilde{\mathbf{R}}_{\hat{\epsilon}\epsilon} = \mathbb{E}[\tilde{\mathbf{r}}_{\hat{\epsilon}\epsilon}(k) \tilde{\mathbf{r}}_{\hat{\epsilon}\epsilon}^T(k)]$ of the signal $\tilde{\mathbf{r}}_{\hat{\epsilon}\epsilon}(k)$ in (6) may be expressed as:

$$\tilde{\mathbf{R}}_{\hat{\epsilon}\epsilon} = \mathbf{F}_N^H \mathbf{R}_{CP} \mathbf{C}_{\hat{\epsilon}}^* \mathbb{E}[\mathbf{r}_\epsilon(k) \mathbf{r}_\epsilon^T(k)] \mathbf{C}_{\hat{\epsilon}}^T \mathbf{R}_{CP}^T \mathbf{F}_N^H, \quad (9)$$

where due to symmetry properties, $\mathbf{C}_{\hat{\epsilon}}^{*T} = \mathbf{C}_{\hat{\epsilon}}^H = \mathbf{C}_{\hat{\epsilon}}^*$ and $\mathbf{F}_N^{HT} = \mathbf{F}_N^H$. Using (7), $\tilde{\mathbf{R}}_{\hat{\epsilon}\epsilon}$ can also be expressed in terms of \mathbf{R}_ϵ as:

$$\tilde{\mathbf{R}}_{\hat{\epsilon}\epsilon} = \mathbf{F}_N^H \mathbf{R}_{CP} \mathbf{C}_{\hat{\epsilon}}^* \mathbf{R}_\epsilon \mathbf{C}_{\hat{\epsilon}}^T \mathbf{R}_{CP}^T \mathbf{F}_N^H. \quad (10)$$

Null or perfectly compensated frequency offset leads to a perfectly orthogonal transmission, and hence to diagonal auto covariance matrices in the frequency domain. Off-diagonal elements in $\tilde{\mathbf{R}}_{\hat{\epsilon}\epsilon}$ are induced by inter-carrier interference and should be minimized.

3.2. Cost function minimizing total off-diagonal power

The goal here is to construct a cost function which penalizes the off-diagonal power of $\tilde{\mathbf{R}}_{\hat{\epsilon}\epsilon}$, for a given offset compensation value $\hat{\epsilon}$. Based on the matrix structure in (10), let us define the matrix function \mathbf{M} of the real scalar μ as:

$$\mathbf{M}(\mu) \triangleq \tilde{\mathbf{R}}_{\hat{\epsilon}\epsilon}|_{\hat{\epsilon}=\mu} = \mathbf{F}_N^H \mathbf{R}_{CP} \mathbf{C}_\mu^* \mathbf{R}_\epsilon \mathbf{C}_\mu^T \mathbf{R}_{CP}^T \mathbf{F}_N^H, \quad (11)$$

where μ is the offset compensation factor, $0 \leq \mu < 1$. The total off-diagonal power $\mathcal{J}(\mu)$ of $\mathbf{M}(\mu)$ may be written as:

$$\mathcal{J}(\mu) = \|\mathbf{M}(\mu) \odot (\mathbf{1}_N - \mathbf{I}_N)\|_F^2, \quad (12)$$

where $\|\cdot\|_F$ denotes the Frobenius norm, \odot is the Hadamard product, $\mathbf{1}_N$ is the $N \times N$ matrix filled with ones and \mathbf{I}_N is the $N \times N$ identity matrix. Finally, the carrier offset estimation problem boils down to finding $\hat{\epsilon}$ such that:

$$\hat{\epsilon} = \arg \min_{\mu} \mathcal{J}(\mu). \quad (13)$$

In the following, \mathcal{J} will act as a cost function, penalizing the off-diagonal energy of \mathbf{M} . Even though the channel matrix \mathbf{H} is unknown to the receiver, the minimization of \mathcal{J} is possible. The right offset compensation value $\hat{\epsilon}$ will force the non-diagonal terms (ICI) of \mathbf{M} to vanish, regardless of the underlying wireless channel.

3.3. Closed-form representation of the cost function

To begin with, let us state the following useful lemma:

Lemma 1. Given any non-zero pseudo-covariance matrix \mathbf{R} of size $P \times P$, and matrices \mathbf{F}_N , \mathbf{R}_{CP} and \mathbf{C}_μ as defined previously in this paper, the function $\mathcal{K}_\mathbf{R}$ of the real parameter μ given by

$$\mathcal{K}_\mathbf{R}(\mu) = \left\| \left(\mathbf{F}_N^H \mathbf{R}_{CP} \mathbf{C}_\mu^* \mathbf{R} \mathbf{C}_\mu^T \mathbf{R}_{CP}^T \mathbf{F}_N^H \right) \odot (\mathbf{1}_N - \mathbf{I}_N) \right\|_F^2$$

can be written as $\mathcal{K}_{\mathbf{R}}(\mu) = A + B \cos(2\pi\mu) + C \sin(2\pi\mu)$, where $A, B, C \in \mathbb{R}$ are specific to the matrix \mathbf{R} .

Proof of Lemma 1 is given in Appendix, as well as the expressions for A, B and C . Choosing $\mathbf{R} = \mathbf{R}_\epsilon$ as defined in (7) we have:

$$\mathcal{J}(\mu) \equiv \mathcal{K}_{\mathbf{R}}(\mu) \big|_{\mathbf{R}=\mathbf{R}_\epsilon} = A_\epsilon + B_\epsilon \cos(2\pi\mu) + C_\epsilon \sin(2\pi\mu), \quad (14)$$

where $A_\epsilon, B_\epsilon, C_\epsilon \in \mathbb{R}$. From (14) we conclude that \mathcal{J} is periodic with period 1 and we can further restrain our analysis to the interval $[0, 1]$. An example of the cost function is depicted in Figure 2. The minimum is reached at the true offset value $\mu \equiv \epsilon = 0.43$. The sinusoidal form may be clearly observed which is in par with the theory.

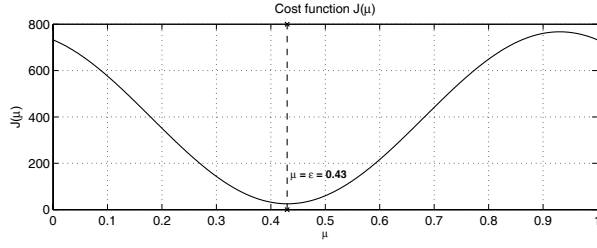


Fig. 2. Cost function $\mathcal{J}(\mu)$, $\epsilon = 0.43$ and SNR=15 dB.

3.4. Algorithm

First, the algorithm computes a sample pseudo-covariance matrix at each time instance k , i.e. $\hat{\mathbf{R}}_\epsilon(k) = \frac{1}{k} \sum_{n=1}^k \mathbf{r}_\epsilon(n) \mathbf{r}_\epsilon^T(n)$. Second, a closed-form minimization of $\mathcal{J}(\mu)$ based on (14) is performed. Evaluating \mathcal{J} at three points within the interval $[0, 1]$ is sufficient to perform the minimization analytically. The extremum points are found to be:

$$\mu_k = \frac{1}{2\pi} \arctan \left\{ \frac{\sqrt{3} (\mathcal{J}(\frac{1}{3}) - \mathcal{J}(\frac{2}{3}))}{2\mathcal{J}(0) - \mathcal{J}(\frac{1}{3}) - \mathcal{J}(\frac{2}{3})} \right\} + \frac{k}{2}, \quad k = 0, 1. \quad (15)$$

Finally the frequency offset estimate yields:

$$\hat{\epsilon} = \arg \min_{k=0,1} \mathcal{J}(\mu_k). \quad (16)$$

4. SIMULATIONS

This section presents the simulation results, using the proposed blind carrier offset estimation algorithm. The OFDM system parameters are chosen as follows: the carrier frequency is $f_0 = 2.4$ GHz, the number of subcarriers is set to $N = 64$ and the available bandwidth is taken equal to $B = 0.5$ MHz. The length L of the cyclic prefix is 4. The subcarrier symbol rate is of 7.8 KHz. The employed symbol modulation is BPSK and the SNR, if not stated otherwise, is equal to 15 dB.

The wireless channel is assumed to experience multipath Rayleigh fading with independent propagation paths. At the beginning of each simulation, a channel impulse response is randomly generated with power loss $[0, -1, -3, -9]$ [dB] and delay profile $[0, 1, 2, 3]$ [μ s], which corresponds to a Typical Urban type of scenario. The channel is then considered to remain constant during one realization of the simulation.

In most of the simulations, independent runs of the algorithm over 200 OFDM blocks are used. This is referred to as a realization. Ensemble averages of the quantities of interest are computed over 100 realizations.

Blind frequency offset estimation over one realization and the associated value of the cost function over time are shown in Figure 3. In this case, the true offset $\epsilon = 0.43$ is found after less than 20 received OFDM blocks. The convergence is rapid even though no virtual subcarriers or pilots are employed in the estimation process. The initial off-diagonal power gets reduced by more than 14 dB. The reduction of the level of inter-carrier interference is depicted in Figure 4 where the pseudo-covariance matrix of the signal in frequency domain is plot before and after compensation for the frequency offset. As shown by Figure 4, accurate offset compensation efficiently removes off-diagonal ICI terms and restores the initial orthogonality of the OFDM transmission.

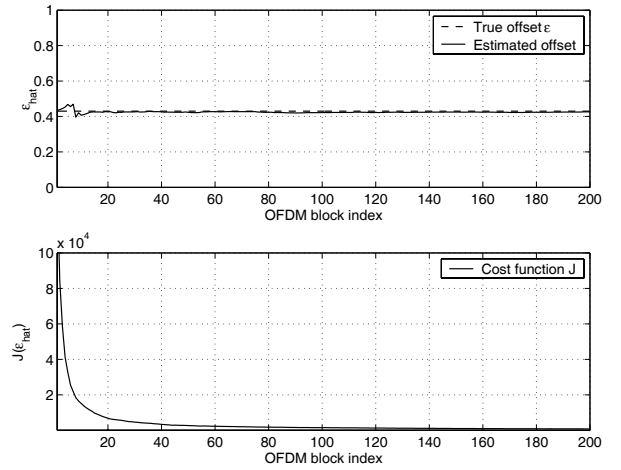


Fig. 3. Estimated frequency offset and cost function over time (1 realization), $\epsilon = 0.43$ and SNR=15 dB.

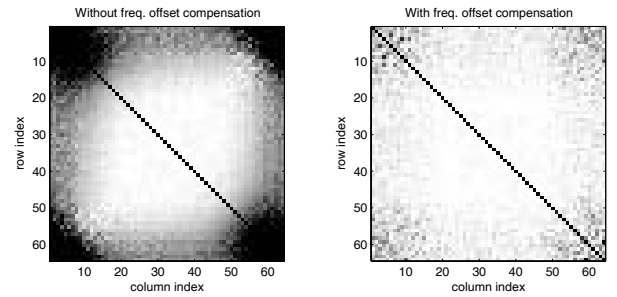


Fig. 4. Pseudo-covariance matrix structure without (on the left) and with (on the right) frequency offset compensation for $\epsilon = 0.43$ and SNR=15 dB. Dark colors correspond to high absolute values. Estimation has been performed over 6000 blocks. Total off-diagonal power gets reduced by 14.5 dB.

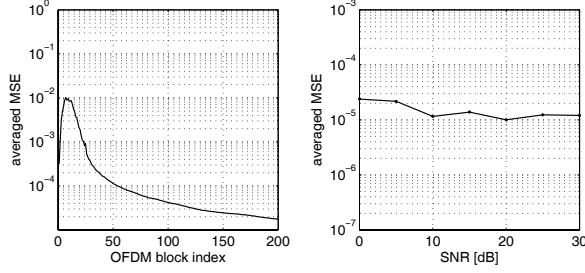


Fig. 5. On the left: MSE vs. number of observed blocks, SNR=5dB. On the right: MSE after convergence vs. SNR. (Ensemble average over 100 realizations, $\epsilon = 0.43$). The performance is almost constant regardless of the SNR.

The Mean Square Error (MSE) is chosen as an error criterion for offset estimation:

$$\text{MSE} = \mathbb{E} |\hat{\epsilon} - \epsilon|^2. \quad (17)$$

Plots of the MSE versus number of observed blocks and SNR are depicted in Figure 5. Convergence is obtained on average after 30 blocks and the MSE reaches 2.10^{-5} at 5 dB SNR after 200 blocks, leaving a residual error less than 1%. The graph of MSE after convergence (200 blocks) as a function of the SNR does not show any significant dependence of the performance on the noise level, as expected, and the MSE remains around 10^{-5} . Note that no virtual subcarriers are exploited here. Hence, the proposed method estimates the offset with high fidelity and the performance remains almost constant regardless of the SNR.

5. CONCLUSIONS

In this paper, a blind frequency offset estimator for OFDM systems was introduced. Since perfect carrier frequency synchronization implies diagonal pseudo-covariance matrix for the received signal, a cost function was designed to enforce such a diagonal structure and thereby estimate the frequency offset. Cost function minimization is accomplished entirely in closed-form. No knowledge of the underlying multipath wireless channel is required. Channel estimation can then be performed as a subsequent step, after frequency synchronization is acquired. The CFO is estimated accurately and the performance remains almost constant regardless of the SNR.

6. APPENDIX

Proof of Lemma 1: First, let us define the matrix $\mathbf{M}(\mu)$ of size $N \times N$ as $\mathbf{M}(\mu) = \mathbf{F}_N^H \mathbf{R}_{CP} \mathbf{C}_\mu^* \mathbf{R}_\mu \mathbf{C}_\mu^T \mathbf{F}_N$, with its general term given by:

$$m_{rs} = \frac{1}{N} e^{\frac{4\pi j L \mu}{N}} \sum_{k=0}^{N-1} \sum_{l=0}^{N-1} e^{-\frac{2\pi j (kr + ls - (k+l)\mu)}{N}} r_{kl}, \quad (18)$$

with $r, s = 0, \dots, N-1$ and where r_{kl} is the (k, l) -th element of the matrix \mathbf{R} of size $P \times P$. Then, \mathcal{K}_R is expressed as:

$$\mathcal{K}_R(\mu) \equiv \|\mathbf{M}(\mu) \odot (\mathbf{I}_N - \mathbf{I}_N)\|_F^2 = \sum_{r=0}^{N-1} \sum_{\substack{s=0 \\ s \neq r}}^{N-1} |m_{rs}|^2. \quad (19)$$

Inserting $|m_{rs}|^2 = m_{rs} m_{rs}^*$ from (18) into (19) and re-arranging terms leads to:

$$\begin{aligned} \mathcal{K}_R(\mu) = & \frac{1}{N^2} \sum_{k=0}^{N-1} \sum_{k'=0}^{N-1} \sum_{l=0}^{N-1} \sum_{l'=0}^{N-1} e^{\frac{2\pi j (k-k'+l-l')\mu}{N}} r_{kl} r_{k'l'}^* \dots \\ & \dots \sum_{r=0}^{N-1} e^{-\frac{2\pi j (k-k')r}{N}} \sum_{\substack{s=0 \\ s \neq r}}^{N-1} e^{-\frac{2\pi j (l-l')s}{N}}. \end{aligned} \quad (20)$$

First, we notice that:

$$\sum_{\substack{s=0 \\ s \neq r}}^{N-1} e^{-\frac{2\pi j (l-l')s}{N}} = \sum_{s=0}^{N-1} e^{-\frac{2\pi j (l-l')s}{N}} - e^{-\frac{2\pi j (l-l')r}{N}}. \quad (21)$$

Second, we recall the following well known result:

$$\forall v \in \mathbb{Z}, \sum_{u=0}^{N-1} e^{j \frac{2\pi uv}{N}} = \begin{cases} N, & \text{if } v = kN, k \in \mathbb{Z}. \\ 0, & \text{otherwise.} \end{cases} \quad (22)$$

Finally, applying (21) and (22) onto (20) provides us with the following closed-form expression for $\mathcal{K}_R(\mu)$:

$$\begin{aligned} \mathcal{K}_R(\mu) = & \sum_{k=0}^{N-1} \sum_{l=0}^{N-1} |r_{kl}|^2 - \frac{1}{N} \sum_{k=0}^{N-1} \sum_{k'=0}^{N-1} \sum_{l=0}^{N-1} \sum_{l'=0}^{N-1} r_{kl} r_{k'l'}^* + \\ & - \frac{2}{N^2} \text{Re} \left\{ \sum_{k=0}^{N-1} \sum_{k'=0}^{N-1} \sum_{l=0}^{N-1} \sum_{l'=0}^{N-1} r_{kl} r_{k'l'}^* \right\} \cos(2\pi\mu) + \dots \\ & - \frac{2}{N^2} \text{Im} \left\{ \sum_{k=0}^{N-1} \sum_{k'=0}^{N-1} \sum_{l=0}^{N-1} \sum_{l'=0}^{N-1} r_{kl} r_{k'l'}^* \right\} \sin(2\pi\mu). \end{aligned}$$

□

7. REFERENCES

- [1] Roman, T., Enescu, M., Koivunen, V., "Joint Time-Domain Tracking of Channel and Frequency Offset for OFDM Systems", in IEEE Workshop on Signal Processing Advances in Wireless Communications, SPAWC 2003, Rome, Italy.
- [2] Chen, B.-S., Tsai, C.-L., "Frequency offset estimation in an OFDM system", IEEE Workshop on Signal Processing Advances in Wireless Communications, 2001. Page(s): 150 - 153.
- [3] Visser, M.A.; Bar-Ness, Y., "Frequency offset correction for OFDM using a blind adaptive decorrelator in a time-variant selective Rayleigh fading channel", Vehicular Technology Conference, 1999 IEEE 49th, Vol.2, May 1999, Page(s): 1281 - 1285.
- [4] Visser, M.A., Pingping Z., Bar-Ness, Y., "A novel method for blind frequency offset correction in an OFDM system", The Ninth IEEE International Symposium on Personal, Indoor and Mobile Radio Communications, Vol.2, Sept. 1998, Page(s): 816 - 820.
- [5] Moose, P.H., "A technique for orthogonal frequency division multiplexing frequency offset correction", IEEE Transactions on Communications, Vol. 42 Issue: 10, Oct. 1994, Page(s): 2908 - 2914.
- [6] Neeser F.D., Massey J.L., "Proper complex random processes with applications to information theory", IEEE Transactions on Information Theory, Vol. 39, Issue: 4, July 1993 Page(s): 1293 -1302.
- [7] Bradaric, I., Petropulu, A.P., "Blind Estimation of the Carrier Frequency Offset in OFDM Systems", 4th IEEE Workshop on Signal Processing Advances in Wireless Communications, SPAWC'03, Rome, Italy, June 2003.